

Dalton Transactions

Accepted Manuscript



This is an *Accepted Manuscript*, which has been through the Royal Society of Chemistry peer review process and has been accepted for publication.

Accepted Manuscripts are published online shortly after acceptance, before technical editing, formatting and proof reading. Using this free service, authors can make their results available to the community, in citable form, before we publish the edited article. We will replace this *Accepted Manuscript* with the edited and formatted *Advance Article* as soon as it is available.

You can find more information about *Accepted Manuscripts* in the [Information for Authors](#).

Please note that technical editing may introduce minor changes to the text and/or graphics, which may alter content. The journal's standard [Terms & Conditions](#) and the [Ethical guidelines](#) still apply. In no event shall the Royal Society of Chemistry be held responsible for any errors or omissions in this *Accepted Manuscript* or any consequences arising from the use of any information it contains.

ARTICLE

DFT studies on the mechanism of palladium-catalyzed carbon–silicon cleavage for the synthesis of benzosilole derivatives†

Cite this: DOI: 10.1039/x0xx00000x

Wen-Jie Chen^a and Zhenyang Lin^{a*}Received 00th January 2012,
Accepted 00th January 2012

DOI: 10.1039/x0xx00000x

www.rsc.org/

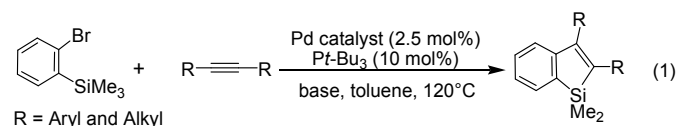
DFT calculations have been carried out to study the detailed mechanism of Pd-catalyzed intermolecular coupling reactions of 2-silylaryl bromides with alkynes via selective cleavage of C(sp³)–Si bonds. Through our calculations, we found that, starting from the alkenylpalladium intermediate derived from oxidative addition of the substrate C–Br bond followed by alkyne insertion, there are two possible pathways leading to the formation of the benzosilole product. Furthermore, these two pathways were found to be competitive. In this paper, we will provide the detailed mechanistic study and analyze the results we have obtained.

Introduction

Cleavage of carbon-silicon bonds is an important process in organic synthesis, especially in metal-catalyzed cross-coupling reactions, because it allows construction of new C–C bonds, leading to new functional molecules.¹ Studies of transition-metal-catalyzed C–Si cleavage reactions have mainly focused on C(sp²)–Si and C(sp)–Si bonds.^{2,3} As for transition-metal-catalyzed cleavage of C(sp³)–Si bonds, early reports were limited to reactions involving either strained silanes (i.e., silacyclopropanes^{1b} and silacyclobutanes⁴) or other activated silanes (e.g., Me₃SiCF₃,⁵ allyl- or benzylsilanes⁶). Reports on transition-metal-catalyzed cleavage of inactivated C(sp³)–Si bonds began to appear in recent years.^{7–12} In 1994, Ojima et al. reported that reaction of diethyl bis(2-butynyl)malonate with HSi^tBuMe₂ catalyzed by rhodium under an atmosphere of CO affords silole derivatives, in which an Me–Si bond from hydrosilane is cleaved.^{7a} In 2011, Matsuda et al. developed an intermolecular variant of Ojima's reaction using disilane, in place of hydrosilane.^{7b} In 2008, Rauf et al. reported the cleavage of a C(sp³)–Si bond in an SiMe₃ group to provide the methyl source for Pd-catalyzed oxidative methylation of olefins.⁸ In 2009, Tobisu et al. reported novel rhodium-catalyzed coupling reactions of 2-trimethylsilylphenylboronic acid with internal alkynes involving cleavage of a C(sp³)–Si bond, which lead to the formation of benzosilole derivatives.⁹ In 2010, Nakao et al. demonstrated that 2-(2-hydroxyprop-2-yl)phenyl-substituted alkylsilanes selectively transfer an alkyl group to facilitate alkylation of aryl halides via cleavage of a

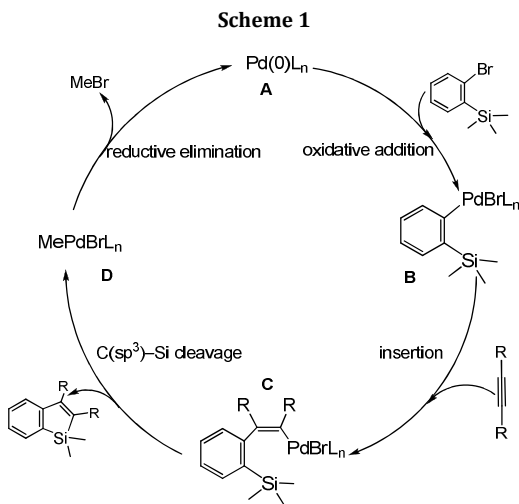
C(sp³)–Si bond.¹⁰ Following Tobisu's pioneering work,^{9a} Liang et al. recently demonstrated that palladium is also a competent catalyst for a similar process.^{11,12} Since the C(sp³)–Si bonds in trialkylsilyl groups are frequently encountered, an efficient and selective cleavage together with further synthetic applications would be very attractive for both mechanistic study and synthetic chemistry.

Very recently, Liang et al. reported facile Pd-catalyzed synthesis of siloles from intermolecular coupling reactions of 2-silylaryl bromides with alkynes via selective cleavage of one of the three C(sp³)–Si bonds (eq. 1).^{11b} A plausible mechanism (Scheme 1) was proposed to account for the reactions. In the proposed mechanism, oxidative addition of the C–Br bond of the substrate 2-trimethylsilylphenyl bromide to Pd(0)L_n generates the intermediate **B**, followed by insertion of alkyne leading to formation of the alkenylpalladium **C**. Then, in **C**, oxidative addition of one Si–Me bond to the Pd(II) center followed by reductive elimination of the benzosilole product gives the MePdBrL_n species **D**. Finally, reductive elimination of MeBr from MePdBrL_n regenerates the active Pd(0)L_n species **A** and completes the catalytic cycle.



However, the detailed mechanism for this coupling reaction is unclear and requires further study. It is interesting

that two possible oxidative additions in **C** exist. One is the oxidative addition of one of the three Si–Me bonds as proposed in Scheme 1. The other one is the oxidative addition of the C(sp²)–Si bond to give a five-membered metallacycle species. In this paper, we explore in details the reaction mechanism for the reactions shown in eq (1) with the aid of density functional theory (DFT) calculations and understand the two possible reaction pathways described above.



Computational Details

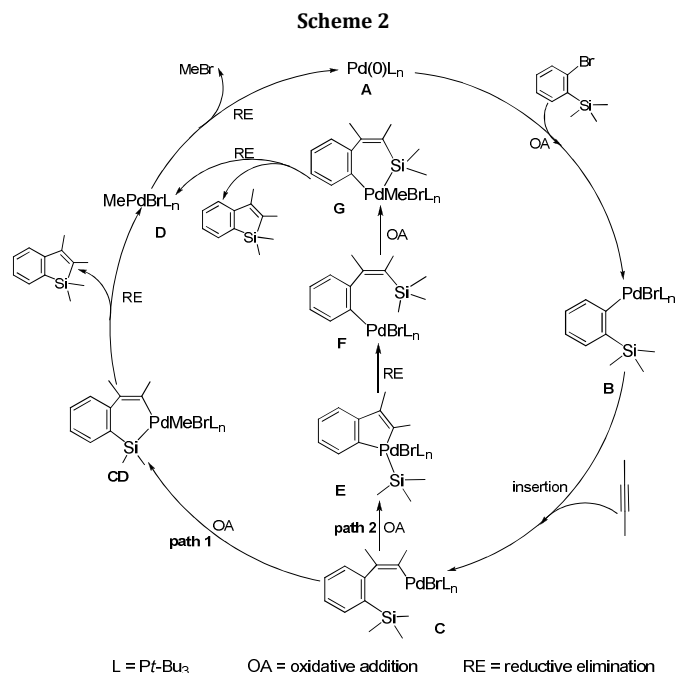
Molecular geometries of the reactants, intermediates, transition states, and products were optimized via density functional theory calculations using the hybrid Becke3LYP (B3LYP) method.¹³ The 6–31G(d) basis set was used for the C and H atoms, while the effective core potentials (ECPs) of Hay and Wadt with double- ζ valance basis set (LanL2DZ)¹⁴ were chosen to describe the Pd, Br, P and Si atoms. In addition, polarization functions were added for Pd(ζ_p) = 1.472, Br(ζ_d) = 0.389, P(ζ_d) = 0.340, Si(ζ_d) = 0.262.¹⁵ Frequency calculations at the same level of theory were carried out to confirm the characteristics of all of the optimized structures as minima (zero imaginary frequencies) or transition states (one imaginary frequency) and to provide free energies at 298.15 K, which include entropic contributions by taking into account the vibrational, rotational, and translational motions of the species under consideration. Calculations of intrinsic reaction coordinates (IRC)¹⁶ were also performed to confirm that transition states connect two relevant minima.

To obtain solvation-corrected relative free energies, we employed a continuum medium to do single-point calculations for all species studied, using UAKS radii on the conductor polarizable continuum model (CPCM).¹⁷ Toluene was employed as the solvent (according to the reaction conditions) in the CPCM calculations. The Gibbs energies in solution, G_{sol} , were calculated by adding the thermodynamic corrections to the CPCM energies (eq (2)).¹⁸ All calculations were performed with the Gaussian 03 software package.¹⁹

$$G_{\text{sol}} = E_{\text{CPCM}} + (G - E) \quad (2)$$

Results and discussion

To better understand the detailed reaction mechanism for the reactions shown in eq (1), we expanded the mechanism shown in Scheme 1 by including the two possible oxidative additions starting from the intermediate **C**. The two related possible catalytic cycles (pathways) are shown in Scheme 2. Path 1 proceeds with oxidative addition of one of the three Si–Me bonds in **C**, leading to the formation of the Pd(IV) species **CD**, followed by reductive elimination of the benzosilole product. Path 2 proceeds with oxidative addition of the Si–Ar bond in **C**, which affords a five-membered metallacycle Pd(IV) species **E**. Subsequent C(alkenyl)–Si bond-forming reductive elimination from **E** results in the formation of the arylpalladium(II) **F**. Then, oxidative addition of one Si–Me bond to the Pd(II) center in **F** gives **G**, from which reductive elimination of the benzosilole product gives the MePdBrL_n species **D**. **D** is the common species for both Paths 1 and 2, from which reductive elimination of MeBr completes the catalytic cycle.



On the basis of the mechanisms shown in Schemes 1 and 2, we first consider the oxidative addition (**A** → **B**) and insertion (**B** → **C**) processes, as shown in Fig. 1. Experimentally, tri-*tert*-butylphosphine (Pt-Bu₃) was used. The bulkiness of Pt-Bu₃ prevents a high coordination number for each palladium species present in the catalytic cycle.²⁰ Therefore, we expect that a monophosphine Pd(0) is the active species. We started with the monophosphine Pd(0) complex **A** in which 2-trimethylsilylphenyl bromide coordinates with the Pd(0) center in an η²-coordination mode, which undergoes oxidative addition via **TS_{A-B}** to afford a three-coordinate species (**B**) with a barrier of 4.8 kcal/mol. The T-shape complex **B**, with the aryl group and Pt-Bu₃ ligand *trans* to each other, isomerizes to another T-shape isomer **B1**, with a very small barrier. The transition state for this isomerization, **TS_{B-B1}**, has a Y-shape structure and lies 2.3 kcal/mol higher in energy than **B**. Then, a ligand substitution of an alkyne molecule for phosphine with an

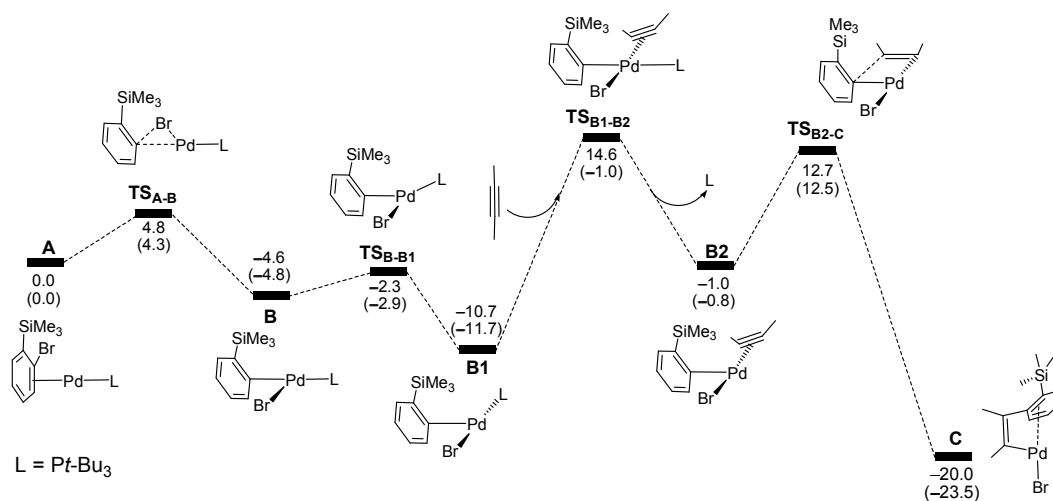


Fig. 1 The energy profile calculated for oxidative addition and insertion processes. The solvation-corrected relative free energies and electronic energies (in parentheses) are given in kcal/mol.

associative mechanism occurs via an approximate square-planar transition state $\text{TS}_{\text{B1-B2}}$. Followed is insertion of alkyne into the Pd–C(aryl) bond in **B2** via the transition state $\text{TS}_{\text{B2-C}}$ to give the intermediate **C** with a barrier of 23.4 kcal/mol. The ligand substitution step is the most energy-demanding from **A** to **C** and the overall free energy barrier was calculated to be 25.3 kcal/mol (the energy of $\text{TS}_{\text{B1-B2}}$ relative to that of **B1** in Figure 1).

We also considered a cationic pathway involving dissociation of bromide from **B** to form $[\text{Pd}(\text{Pt-Bu}_3)(\text{silylaryl})(\text{alkyne})]^+$ for alkyne insertion. The bromide dissociation barrier was calculated to be 65.5 kcal/mol, which is inaccessible high.

In the following sections, our main objective is to obtain deep insight into the oxidative addition of $\text{C}(\text{sp}^3)\text{-Si}$ versus $\text{C}(\text{sp}^2)\text{-Si}$ to a palladium(II) metal center. We investigated associative and dissociative mechanisms considering whether Pt-Bu_3 stays attached to the metal center from the complex **C** to **D** in Paths 1 and 2. We found that a dissociative mechanism is much more favorable. Fig. 2 shows the free energy profiles calculated for Paths 1 and 2 involving a dissociative mechanism. The corresponding free energy profiles involving an associative mechanism (less favorable) are given in the Supplementary Information.

In Path 1, oxidative addition of one of the three $\text{Si-C}(\text{sp}^3)$ bonds in **C**, which is π -coordinated η^2 -aryl species, via the transition state $\text{TS}_{\text{C-CD}}$ occurs to give the six-membered ring intermediate **CD**, with a barrier of 19.6 kcal/mol. (Fig. 2(a)) $\text{TS}_{\text{C-CD}}$ represents the transition state connecting a slightly distorted T-shape Pd(II) complex (**C**) and a seesaw Pd(IV) structure (**CD**). The complex **CD**, with the methyl and bromide ligands *trans* to each other, isomerizes to another seesaw isomer **CD1** with a very small barrier of 1.2 kcal/mol. Then reductive elimination in **CD1** via $\text{TS}_{\text{CD1-D}}$ leads to dissociation of the benzosilole product molecule, and the Pt-Bu_3 ligand association readily gives the MePdBrL **D**. $\text{CD1} \rightarrow \text{D}$ is a two-step, energy downhill process. In this path, the highest-energy transition state $\text{TS}_{\text{C-CD}}$ was calculated for the oxidative addition step, and the overall barrier for the process from **C** to **D** was calculated to be 19.6 kcal/mol.

In Path 2 (Fig. 2(b)), from the complex **C**, oxidative addition of the Si-Ar bond occurs to afford the five-membered

metallacycle Pd(IV) species **E**, with a barrier of 7.0 kcal/mol. Subsequent C(alkenyl)–Si bond-forming reductive elimination in **E** produces the T-shape arylpalladium(II) complex **F** via the transition state $\text{TS}_{\text{E-F}}$, which is calculated to lie slightly higher in energy than $\text{TS}_{\text{C-E}}$. The T-shape, π -coordinated arylpalladium(II) complex **F** isomerizes to a C–H agostic intermediate (**F1**) with a barrier of 13.3 kcal/mol. Then, oxidative addition of one Si-Me bond to the Pd(II) center gives **G** via the transition state $\text{TS}_{\text{F1-G}}$, followed by reductive elimination of the benzosilole product via the transition state $\text{TS}_{\text{G-D}}$ and the Pt-Bu_3 ligand association to give MePdBrL species **D**. $\text{G} \rightarrow \text{D}$ is also a two-step, energy downhill process. $\text{TS}_{\text{F1-G}}$ is the highest-energy transition state for this path (Path 2) from **C** to **D** and the barrier is calculated to be 23.1 kcal/mol (the energy of $\text{TS}_{\text{F1-G}}$ relative to that of **F** in Fig. 2(b)). The calculated energy profiles (Fig. 2) show that Path 1 is slightly more favorable than Path 2.

It is important to note that Path 1 involves oxidation addition followed by reductive elimination (OA/RE), $\text{Pd(II)} \rightarrow \text{Pd(IV)} \rightarrow \text{Pd(II)}$ ($\text{C} \rightarrow \text{CD/CD1} \rightarrow \text{D}$). The OA/RE process involves a $\text{C}(\text{sp}^3)\text{-Si}$ bond cleavage (OA) and a $\text{C}(\text{sp}^2)\text{-Si}$ bond formation (RE). Path 2 involves two such processes, $\text{Pd(II)} \rightarrow \text{Pd(IV)} \rightarrow \text{Pd(II)} \rightarrow \text{Pd(IV)} \rightarrow \text{Pd(II)}$ ($\text{C} \rightarrow \text{E} \rightarrow \text{F}$ and $\text{F1} \rightarrow \text{G} \rightarrow \text{D}$). In the first OA/RE process $\text{C} \rightarrow \text{E} \rightarrow \text{F}$, a $\text{C}(\text{sp}^2)\text{-Si}$ bond is cleaved (OA) and a new $\text{C}(\text{sp}^2)\text{-Si}$ bond is formed (RE) while in the second OA/RE process $\text{F1} \rightarrow \text{G} \rightarrow \text{D}$, a $\text{C}(\text{sp}^3)\text{-Si}$ bond is cleaved (OA) and a $\text{C}(\text{sp}^2)\text{-Si}$ bond is formed (RE). Among the three OA/RE processes, $\text{C} \rightarrow \text{E} \rightarrow \text{F}$ is the most facile. These results are consistent with notion that oxidative addition of $\text{C}(\text{sp}^3)\text{-Si}$ versus $\text{C}(\text{sp}^2)\text{-Si}$ shows normally a preference for the latter.^{1a,1c-1f,2a,2g} The reason for the OA/RE process $\text{C} \rightarrow \text{E} \rightarrow \text{F}$ being the most facile is also closely related to the fact that among the four Pd(IV) species **CD**, **CD1**, **E** and **G** (Fig. 2), **E** is the most stable. We can also conveniently attribute the high stability of **E**, when compared with **CD**, **CD1** and **G**, to the fact that there are two strong Pd(IV)– $\text{C}(\text{sp}^2)$ bonds in **E** while in the other two each have only one Pd(IV)– $\text{C}(\text{sp}^2)$ bond. In addition, through the energy profiles in Fig. 2 we can see that $\text{TS}_{\text{C-CD}}$ and $\text{TS}_{\text{F1-G}}$, both of which involve $\text{C}(\text{sp}^3)\text{-Si}$ bond cleavage, were calculated to be the highest transition states for Paths 1 and 2, respectively. Interestingly, the transition state $\text{TS}_{\text{C-CD}}$ and the intermediate

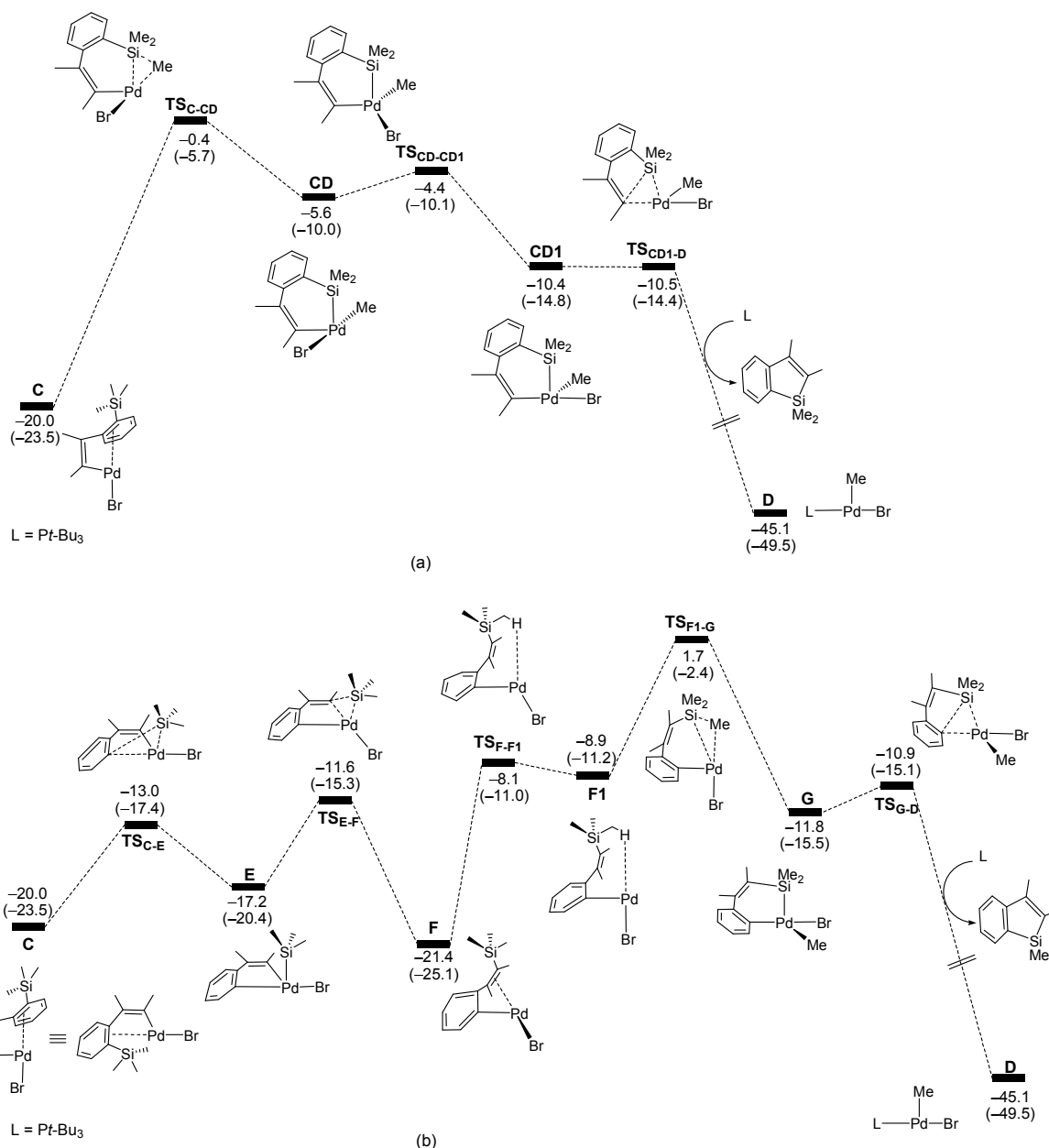


Fig. 2 The energy profiles calculated for Paths 1 (a) and 2 (b). The solvation-corrected relative free energies and electronic energies (in parentheses) are given in kcal/mol.

CD1 in Fig. 2(a) show similar stabilities to the transition state **TS_{F1-G}** and the intermediate **G** in Fig. 2(b), respectively. The structures of **TS_{C-CD}** versus **TS_{F1-G}** and **CD1** versus **G** differ only in the relative positions of the phenyl ring and the olefinic moiety in the bidentate ligands, indicating that both Paths 1 and 2 are competitive and possible for the process from **C** to **D**. In a recent theoretical study on the related Rh-catalyzed coupling of 2-trimethylsilylphenylboronic acid with internal alkynes, two reaction pathways similar to Paths 1 and 2 have been studied and the same conclusion regarding the preference of the reaction pathways has also been made.²¹

Fig. 3 shows the optimized structures with selected structural parameters for the species relevant in the two paths studied. Examination of the bond distances indicates the following: (i) Both the transition states **TS_{C-CD}** and **TS_{F1-G}** show

cleavage of a C(sp³)-Si bond. The C(sp³)-Si distances, which are 1.89 Å in complex **C** and 1.90 Å in complex **F1**, increase respectively to 2.21 Å in **TS_{C-CD}** and to 2.20 Å in **TS_{F1-G}**. For the C(sp²)-Si bond cleavage process **C** → **E** which involves the transition state **TS_{C-E}**, the C-Si distance increases from 1.92 Å in complex **C** to 2.27 Å in **TS_{C-E}**. (ii) In the complex **F1**, the distance between the palladium and the nearest hydrogen atom is 2.21 Å, which is a prime indicator for the presence of an agostic Pd...H interaction. The oxidative addition process via the transition state **TS_{F1-G}** needs to pass through **F1**, instead of directly from **F**, due to that the cleaved Si-C bond is closer to the metal center in **F1** than in **F**.

From the intermediate **D**, reductive elimination occurs to give MeBr via a three-membered transition state **TS_{D-A}** with a barrier of 30.2 kcal/mol (Fig. 4). After releasing one MeBr

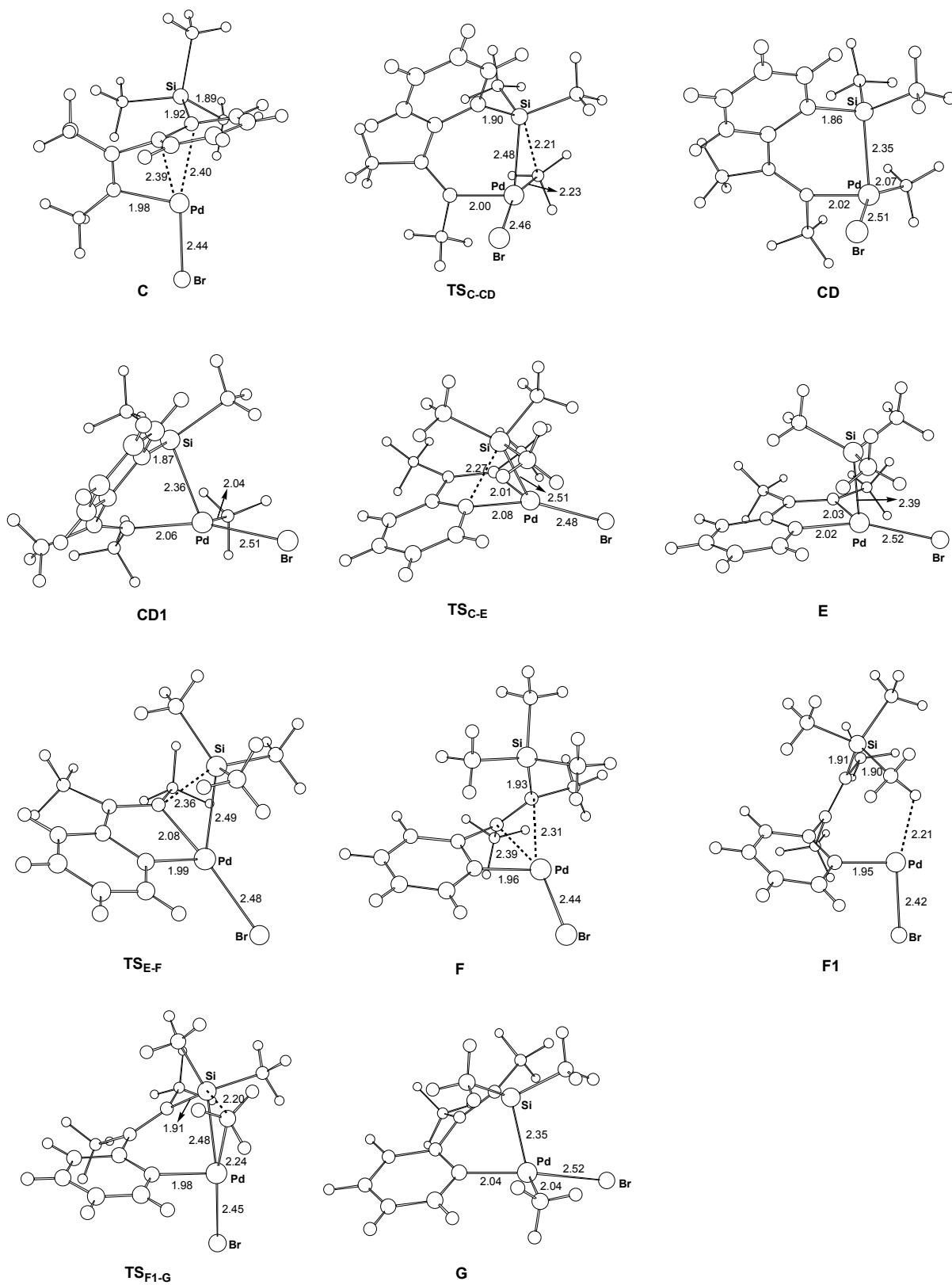


Fig. 3 Optimized structures and transition states for the selected species involved in the pathways related to **Fig. 1**. Selected structural parameters are given (bond length in Å).

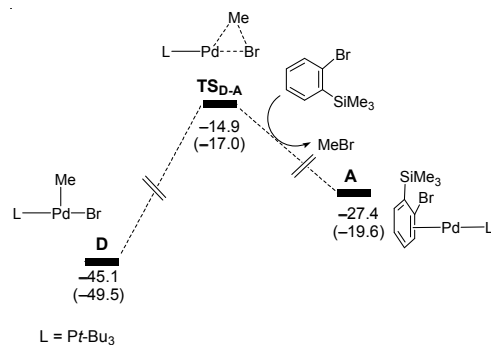


Fig. 4 The energy profile calculated for the regeneration of active species A. The solvation-corrected relative free energies and electronic energies (in parentheses) are given in kcal/mol.

molecule, the active catalytic species **A** is regenerated to complete the catalytic cycle. Comparing the energy profiles in Figures 1, 2 and 4, we see that the reductive elimination in Fig. 4 is theoretically predicted to be the rate-determining step. The rate-determining barrier of 30.2 kcal/mol is high, consistent with experimental condition of 120 °C.^{11b}

Conclusions

The reaction mechanism of palladium-catalyzed intermolecular coupling reactions of 2-silylaryl bromides with alkynes via selective cleavage of C(sp³)-Si bonds has been investigated with the aid of DFT calculations. The computational results are consistent with a catalytic cycle that includes: (1) oxidative addition of C-Br bond to yield an arylpalladium intermediate, (2) insertion of alkyne leading to formation of the alkenylpalladium, (3) oxidative addition of one Si-Me bond to the Pd(II) center followed by reductive elimination of the benzosilole product gives the MePdBrL_n species, (4) reductive elimination of MeBr from MePdBrL_n regenerates the active Pd(0)L_n species. The reductive elimination in step (4) is theoretically predicted to be the rate-determining step.

Careful study of the above-mentioned step (3) leads us to find an alternative pathway to complete this step. This alternative pathway involves two processes of oxidative addition followed by reductive elimination (OA/RE). In the first OA/RE process, oxidative addition of C(sp²)-SiMe₃ (instead of one Si-Me bond) gives a five-membered-ring Pd(IV) metallocycle containing a SiMe₃ ligand and reductive elimination leads to the formation of a Pd(II) species containing a ((trimethylsilyl)alkenyl)phenyl ligand. In the second OA/RE process, from the Pd(II) species oxidative addition of one Si-Me bond occurs followed by reductive elimination to complete this step.

From our calculations, we found that oxidative addition of C(sp²)-Si to a Pd(II) center is easier than that of C(sp³)-Si, which is the main reason for the existence of the alternative pathway for step (3). In both the pathways, oxidative addition of C(sp³)-Si to Pd(II) is the most energy-demanding. As both pathways undergo oxidative addition of C(sp³)-Si to Pd(II), the two pathways are found to be competitive with comparable barriers.

Our calculation results indicate that Pt-Bu₃ is not involved in step (3) due to the fact that the phosphine ligand is extremely

bulky. Therefore, it is expected that there are on and off events associated with the phosphine ligand binding in the whole catalytic cycle. Because of these on-and-off events, it is expected that presence of more phosphine ligands would make the catalytic process efficient. Indeed, 2.5 mol% of Pd catalyst and 10 mol% of Pt-Bu₃ ligand were included in the optimized reaction conditions.

Acknowledgements

This work was supported by the Research Grants Council of Hong Kong (HKUST603313 and CUHK7/CRF/12G).

^a Department of Chemistry, The Hong Kong University of Science and Technology, Clear Water Bay, Kowloon, Hong Kong, People's Republic of China. E-mail: chzlin@ust.hk

† Electronic Supplementary Information (ESI) available: Complete Reference for Ref. 19, the energy profiles calculated for Paths 1 and 2 with associative mechanism and Cartesian coordinates and total energies for all of the calculated structures. See DOI: 10.1039/b000000x/

References

- (a) T. Hiyama, In *Metal-Catalyzed Cross-Coupling Reactions*; Diederich, F., Stang, P. J., Eds.; Wiley-VCH: Weinheim, Germany, 1998, pp. 421–453. (b) A. K. Franz, K. A. Woerpel, *Acc. Chem. Res.* 2000, **33**, 813. (c) S. E. Denmark, R. F. Sweiss, *Acc. Chem. Res.* 2002, **35**, 835. (d) A. C. Spivey, C. J. G. Gripton, J. P. Hannah, *Curr. Org. Synth.* 2004, **1**, 211. (e) S. E. Denmark, R. F. Sweis, In *Metal-Catalyzed Cross-Coupling Reactions*; A. de Meijere, F. Diederich, Eds. (Second Edition); Wiley-VCH Verlag GmbH: Weinheim, Germany, 2008, pp. 163–216. (f) W. Rauf, A. Hazari, V. Gouverneur, J. M. Brown, *Pure Appl. Chem.* 2010, **82**, 1415.
- For selected examples of transition-metal-catalyzed cleavage of C(sp²)-Si bonds, see: (a) Y. Nakao, H. Imanaka, A. K. Sahoo, A. Yada, T. Hiyama, *J. Am. Chem. Soc.* 2005, **127**, 6952. (b) E. Alacid, C. Nájera, *Adv. Synth. Catal.* 2006, **348**, 2085. (c) S. Yang, B. Li, X. Wan, Z. Shi, *J. Am. Chem. Soc.* 2007, **129**, 6066. (d) X. Dai, N. A. Strotman, G. C. Fu, *J. Am. Chem. Soc.* 2008, **130**, 3302. (e) L. Zhang, J. Wu, *J. Am. Chem. Soc.* 2008, **130**, 12250. (f) S. Tang, M. Takeda, Y. Nakao, T. Hiyama, *Chem. Commun.* 2011, **47**, 307. (g) K. Matsumoto, M. Shindo, *Adv. Synth. Catal.* 2012, **354**, 642.
- For selected examples of transition-metal-catalyzed cleavage of C(sp)-Si bonds, see: (a) M. J. Wu, L. M. Wei, C. F. Lin, S. P. Leou, L. L. Wei, *Tetrahedron* 2001, **57**, 7839. (b) W. J. Sommer, M. Weck, *Adv. Synth. Catal.* 2006, **348**, 2101. (c) A. Horita, H. Tsurugi, T. Satoh, M. Miura, *Org. Lett.* 2008, **10**, 1751. (d) H. Huang, H. Liu, H. Jiang, K. Chen, *J. Org. Chem.* 2008, **73**, 6037. (e) N. Sakai, R. Komatsu, N. Uchida, R. Ikeda, T. Konakahara, *Org. Lett.* 2010, **12**, 1300.
- K. Hirano, H. Yorimitsu, K. Oshima, *Chem. Commun.* 2008, 3234.
- (a) J. E. Cho, T. D. Senecal, T. Kinzel, Y. Zhang, D. A. Watson, S. L. Buchwald, *Science* 2010, **328**, 1679. (b) L. Chu, F. L. Qing, *Org. Lett.* 2010, **12**, 5060. (c) L. Chu, F. L. Qing, *J. Am. Chem. Soc.* 2010, **132**, 7262.

- 6 (a) I. Fleming, A. Barbero, D. Walter, *Chem. Rev.* 1997, **97**, 2063. (b) C. Mateo, C. Fernández-Rivas, A. M. Echavarren, D. J. Cárdenas, *Organometallics* 1997, **16**, 1997. (c) T. Matsuda, S. Kadowaki, Y. Yamaguchi, M. Murakami, *Chem. Commun.* 2008, 2744.
- 7 (a) I. Ojima, D. A. Fracchiolla, R. J. Donovan, P. Banerji, *J. Org. Chem.* 1994, **59**, 7594. (b) T. Matsuda, Y. Suda, Y. Fujisaki, *Synlett* 2011, 813.
- 8 W. Rauf, J. M. Brown, *Angew. Chem., Int. Ed.* 2008, **47**, 4228.
- 9 (a) M. Tobisu, M. Onoe, Y. Kita, N. Chatani, *J. Am. Chem. Soc.* 2009, **131**, 7506. (b) M. Onoe, K. Baba, Y. Kim, Y. Kita, M. Tobisu, N. Chatani, *J. Am. Chem. Soc.* 2012, **134**, 19477.
- 10 Y. Nakao, M. Takeda, T. Matsumoto, T. Hiyama, *Angew. Chem., Int. Ed.* 2010, **49**, 4447.
- 11 (a) Y. Liang, S. Zhang, Z. Xi, *J. Am. Chem. Soc.* 2011, **133**, 9204. (b) Y. Liang, W. Geng, J. Wei, Z. Xi, *Angew. Chem., Int. Ed.* 2012, **51**, 1934.
- 12 T. H. Meng, K. B. Ouyang, Z. Xi, *RSC Adv.* 2013, **3**, 14273.
- 13 (a) A. D. Becke, *J. Chem. Phys.* 1993, **98**, 5648. (b) B. Miehlich, A. Savin, H. Stoll, H. Preuss, *Chem. Phys. Lett.* 1989, **157**, 200. (c) C. Lee, W. Yang, G. Parr, *Phys. Rev. B.* 1988, **37**, 785. (d) P. J. Stephens, F. J. Devlin, C. F. Chaobalowski, *J. Phys. Chem.* 1994, **98**, 11623.
- 14 (a) W. R. Wadt, P. J. Hay, *J. Chem. Phys.* 1985, **82**, 284. (b) P. J. Hays, W. R. Wadt, *J. Chem. Phys.* 1985, **82**, 299.
- 15 (a) A. W. Ehlers, M. Böhme, S. Dapprich, A. Gobbi, A. Höllwarth, V. Jonas, K. F. Köhler, R. Stegmann, G. Frenking, *Chem. Phys. Lett.* 1993, **208**, 111. (b) A. Höllwarth, M. Böhme, S. Dapprich, A. W. Ehlers, A. Gobbi, V. Jonas, K. F. Köhler, R. Stegmann, A. Veldkamp, G. Frenking, *Chem. Phys. Lett.* 1993, **208**, 237. (c) S. Huzinaga, *Gaussian Basis Sets for Molecular Calculations*; Elsevier Science Pub. Co.: Amsterdam, 1984.
- 16 (a) K. Fukui, *J. Phys. Chem.* 1970, **74**, 4161. (b) K. Fukui, *Acc. Chem. Res.* 1981, **14**, 363.
- 17 (a) M. Cossi, N. Rega, G. Scalmani, V. Barone, *J. Comput. Chem.* 2003, **24**, 669. (b) M. Cossi, V. Barone, R. Cammi, J. Tomasi. *Chem. Phys. Lett.* 1966, **255**, 327. (c) M. Cossi, V. Barone, B. Mennucci, J. Tomasi, *Chem. Phys. Lett.* 1988, **286**, 253. (d) M. Cossi, V. Barone, M. A. Robb, *J. Chem. Phys.* 1999, **111**, 5295.
- 18 (a) D. Balcells, G. Ujaque, I. Fernandez, N. Khiar, F. Maseras, *J. Org. Chem.* 2006, **71**, 6388. (b) A. A. C. Braga, G. Ujaque, F. Maseras, *Organometallics* 2006, **25**, 3647.
- 19 M. J. Frisch, et al. Gaussian 03, revision E. 01; Gaussian, Inc., Wallingford CT, 2004.
- 20 J. F. Hartwig, F. Paul, *J. Am. Chem. Soc.*, 1995, **117**, 5373. (b) J. P. Stambuli, M. Bühl, J. F. Hartwig, *J. Am. Chem. Soc.*, 2002, **124**, 9346.
- 21 Z. Y. Yu, Y. Lan, *J. Org. Chem.* 2013, **78**, 11501.

DFT studies on the mechanism of palladium-catalyzed carbon-silicon cleavage for the synthesis of benzosilole derivatives†

Wen-Jie Chen^a and Zhenyang Lin^{a*}

DFT calculations have been carried out to study the detailed mechanism of Pd-catalyzed intermolecular coupling reactions of 2-silylaryl bromides with alkynes via selective cleavage of C(sp³)-Si bonds.

